

Climate warming accelerates carbon release from foliar litter—A global synthesis

Zihao Chen^{1,2}  | Xiangyin Ni^{1,2}  | Guillaume Patoine^{3,4}  | Changhui Peng⁵  |
 Kai Yue^{1,2}  | Ji Yuan^{1,2}  | Qiuxia Wu^{1,2} | Nico Eisenhauer^{3,4}  |
 Carlos A. Guerra^{3,4}  | Roland Bol⁶  | Fuzhong Wu^{1,2}  | G. Geoff Wang⁷ 

¹Key Laboratory for Humid Subtropical Eco-Geographical Processes of the Ministry of Education, School of Geographical Sciences, Fujian Normal University, Fuzhou, China

²Fujian Sanming Forest Ecosystem National Observation and Research Station, Sanming, China

³German Centre for Integrative Biodiversity Research (iDiv) Halle-Jena-Leipzig, Leipzig, Germany

⁴Institute of Biology, Leipzig University, Leipzig, Germany

⁵Institute of Environment Sciences, University of Quebec at Montreal, Montreal, Quebec, Canada

⁶Institute of Bio- and Geosciences, Agrosphere (IBG-3), Forschungszentrum Jülich, Jülich, Germany

⁷Department of Forestry and Environmental Conservation, Clemson University, Clemson, South Carolina, USA

Correspondence

Fuzhong Wu, Key Laboratory for Humid Subtropical Eco-Geographical Processes of the Ministry of Education, School of Geographical Sciences, Fujian Normal University, Fuzhou, China.
 Email: wufzchina@fjnu.edu.cn

Funding information

National Natural Science Foundation of China, Grant/Award Number: 32022056 and 32171641; National Key R&D Program of China, Grant/Award Number: 2023YFF1305500; German Research Foundation, Grant/Award Number: 202548816, Ei 862/29-1 and Ei 862/31-1

Abstract

With over one-third of terrestrial net primary productivity transferring to the litter layer annually, the carbon release from litter serves as a crucial valve in atmospheric carbon dioxide concentrations. However, few quantitative global projections of litter carbon release rate in response to climate change exist. Here, we combined a global foliar litter carbon release dataset (8973 samples) to generate spatially explicitly estimates of the response of their residence time (τ) to climate change. Results show a global mean litter carbon release rate (k) of 0.69 year^{-1} (ranging from $0.09\text{--}5.6 \text{ year}^{-1}$). Under future climate scenarios, global mean τ is projected to decrease by a mean of 2.7% (SSP 1–2.6) and 5.9% (SSP 5–8.5) during 2071–2100 period. Locally, the alleviation of temperature and moisture restrictions corresponded to obvious decreases in τ in cold and arid regions, respectively. In contrast, τ in tropical humid broadleaf forests increased by 4.6% under SSP 5–8.5. Our findings highlight the vegetation type as a powerful proxy for explaining global patterns in foliar litter carbon release rates and the role of climate conditions in predicting responses of carbon release to climate change. Our observation-based estimates could refine carbon cycle parameterization, improving projections of carbon cycle–climate feedbacks.

KEY WORDS

carbon release, carbon residence time, climate change, litter decomposition, vegetation type

1 | INTRODUCTIONS

Litter carbon release is a key ecological process that links carbon cycling between land and atmosphere, with this carbon flux representing the crucial counterpart to carbon uptake by photosynthesis in terrestrial ecosystems (Berg & McClaugherty, 2014; Li et al., 2019). Carbon released from litter decomposition through soil microbial metabolism either enters the atmosphere as carbon dioxide (CO_2) or is transferred into the soil carbon pool for subsequent turnover and storage. (Bradford et al., 2016; Cotrufo et al., 2013; Parton et al., 2007). As such, the rate of litter carbon release partly determines the terrestrial carbon balance and its feedback to climate change. The observation and prediction of litter mass and nutrient loss have been enduring topics (Djukic et al., 2018; Lajtha et al., 2018; Parton et al., 2007), with many conceptual and mechanistic models being proposed and applied (Olson, 1963; Parton et al., 1993; Rovira & Rovira, 2010; Tuomi et al., 2009). However, a notable gap persists in obtaining accurate estimates of the global-scale litter carbon release rate and its covariation with climate, leading to significant uncertainty in the future climate forecasts using Earth system models.

On the one hand, many well-established empirical models cannot be robustly extrapolated to broader spatial scales, because they are constrained by the specific litter type or ecosystem under investigation (Rovira & Rovira, 2010; Tuomi et al., 2009). On the other hand, in current top-down models, the simple constant parameterization (e.g., the mean of the lignin-to-nitrogen ratio of different litter) of litter carbon release rates, fails to match natural vegetation distributions, which inevitably introduces biases into carbon cycle predictions (Farina et al., 2013; Luo & Schuur, 2020). Simulations that rely on the mean correlations of litter quality indices and carbon turnover may overlook the carbon flux originating from litter components with significantly different individual turnover times, especially across diverse climate gradients and vegetation types (Pan et al., 2011; Pietsch et al., 2014). Furthermore, climate takes the spotlight in the conceptual framework of litter decay studies (Berg, 2014; García-Palacios et al., 2013; Joly et al., 2023), as it accounts for the majority of the variation in litter decomposition, forming the foundation of the hierarchical model (Joly et al., 2023; Swift et al., 1979). Because the relationship between climate and residence time of litter carbon remains debated (Bradford et al., 2017; Portillo-Estrada et al., 2016), it becomes difficult to predict the direction or magnitude of warming-induced changes in the litter carbon release rate.

Machine-learning approaches may help address these challenges because they can effectively deal with geodata and describe the spatial patterns in ecological processes with convincing accuracy (Hengl et al., 2017; Pichler & Hartig, 2023). Unlike process-oriented models, geospatial modeling with a georeferenced observational dataset as input uses a composite predictor layer to extract environmental information for training a model and creating spatial-explicit predictions (Cai et al., 2023; Patoine et al., 2022). By following this pipeline, the rate of litter carbon release as an integrative metric of the decomposition process can be predicted, providing fundamental biogeographic insights without considering the intricate mechanistic

biochemistry involved. Approximately 80% of the foliar litter carbon decays rapidly (within months to years) and the remaining carbon enters the soil system (Prescott, 2010). To address the critical knowledge gap described above, we examine the regulators of the release rate of foliar litter carbon and extrapolate these relationships at the global scale.

Here, we used a comprehensive dataset of 8973 foliar litter carbon release samples from all terrestrial vegetation types (Figure 1a; Figure S1) and 20 environmental predictors (Table S1) to train three machine-learning approaches including Random Forests (RF), Gradient Boosting Machine (GBM), and Extreme Gradient Boosting (XGB) models and generated global predictions of carbon release rate. These three models achieved strong predictive performance (based on 10-fold cross-validation, Table S2), and their predicted values correlated well with the observed foliar litter carbon rates, demonstrating high accuracy in most regions of the globe (Figures S2 and S3). The robust predictive capability of these models facilitated the extension of complex relationships between decomposition rate and environmental factors to the global scale. Finally, we applied our well-tested machine-learning models to project potential changes in rate of foliar litter carbon under future climate change scenarios provided by the Coupled Model Intercomparison Project Phase 6 (CMIP6) climate models for Shared Socioeconomic Pathway (SSP) scenarios 1–2.6 (sustainable, low-carbon emissions) and 5–8.5 (very high greenhouse gas emissions) (Eyring et al., 2016; Karger et al., 2017).

2 | MATERIALS AND METHODS

2.1 | Data integration

We searched for peer-reviewed articles, academic theses, and book chapters, published in English or Chinese before December 2022, in Web of Science (WoS; www.webofscience.clarivate.cn) and China National Knowledge Infrastructure (CNKI; www.cnki.net), with the following search string ("litter decomposition" OR "litter decay" OR "litter breakdown" OR "litter degradation" OR "litter mass loss" OR "litter release") AND ("foliar" OR "leaf" OR "foliage" OR "leafage" OR "broadleaf" OR "broadleaved" OR "needle" OR "coniferous") and their equivalents in Chinese. Studies were included in foliar litter carbon release dataset if they complied with the following criteria: (1) All data were obtained from decomposition experiments conducted on terrestrial soils, excluding aquatic systems, wetlands, rivers, and lakes. (2) Measurement of foliar litter decomposition, excluding wood, bark, or artificial substrates, was conducted in natural field sites using *in situ* litterbags or tubes without any specific treatments, such as manipulation of temperature, precipitation, nitrogen addition, atmospheric CO_2 , or decomposers. (3) Studies reported information on longitude and latitude, species names, vegetation type, and mesh size ($\geq 1\text{ mm}$) of litterbags. The use of a mesh size of $\geq 1\text{ mm}$ allows the entry of all mesofauna (Bradford et al., 2002; Wang et al., 2015). (4) Foliar types used for decomposition corresponded

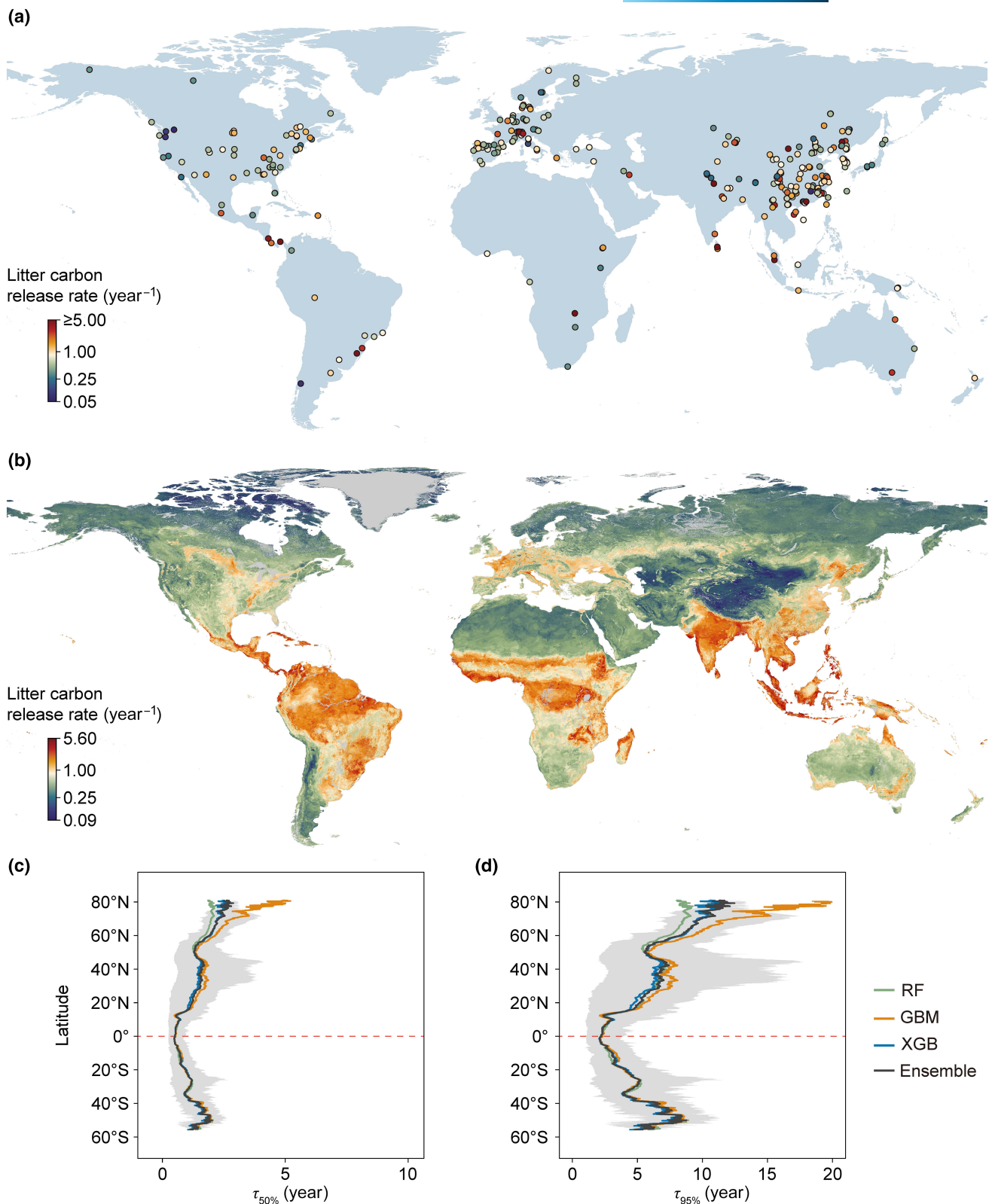


FIGURE 1 The global distribution of foliar litter carbon release observations and ensemble prediction. (a) Map of foliar litter decomposition studies included in our dataset. (b) Foliar litter carbon release rate based on ensemble prediction of three different models (GBM, gradient boosting machine; RF, random forest; XGB, extreme gradient boosting) weighted by model accuracy. (c, d) Latitudinal patterns of $\tau_{50\%}$ and $\tau_{95\%}$ based on three models and ensemble.

to the typical vegetation types found in the plots. Litterbags exclusively contained a single plant species unless designated for mixed samples in needle-broadleaf mixed forest vegetation types. (5) For cropland, given the practice of straw incorporation in production management, most crop residues decompose underground. Therefore, we did not distinguish data from cropland experiments conducted in topsoil and subsoil. Based on these criteria, a total of 8973 time series observations from 1840 decomposition experiments, encompassing every continent except Antarctica, were used for geospatial statistical analyses (Figure 1a; Figure S1).

2.2 | Foliar litter carbon release rate and residence time

The foliar litter carbon release rate is calculated using the widely employed single exponential decomposition model. The assumption of the single exponential model is that the decomposition constant remains constant throughout the decomposition process, and the litter will decompose completely. Although the decomposition rate of litter may vary across stages and there might be a limit to mass loss (Berg, 2014), the concept of decomposition resistance is also contentious (Lehmann & Kleber, 2015). Therefore, mechanistically assessing the decomposition rates across different stages poses a challenge. The single exponential model represents a gross simplification of complex processes, but it offers the advantage of being an efficient and straightforward method for comparing turnover times on a large spatial scale (Berg, 2014; Prieto et al., 2019). The single exponential model was elaborated by Olson (1963):

$$m_t / m_0 = e^{-kt}, \quad (1)$$

in which m_t is the litter carbon mass at a certain sampling time (t), m_0 is the initial litter carbon mass, k is the carbon release rate constant (year^{-1}). We calculated k for samples with three or more samplings and retained k values with fitted R^2 greater than .6. Next, we calculated the residence time (τ) required for the release of 50% ($\tau_{50\%}$, year) and 95% ($\tau_{95\%}$, year) of litter carbon mass in each experiment:

$$\tau_{50\%} = -\ln(0.5) / k, \quad (2)$$

and

$$\tau_{95\%} = -\ln(0.05) / k, \quad (3)$$

2.3 | Global environmental variables

To construct predictive models of foliar litter carbon release rate, we first extracted values from our prepared stack of 20 ecologically relevant, global environmental variables (Table S1) for each independent point location. These predictors included variables describing climate, soil physics, soil chemistry, vegetative indices, soil microbes, and topography (Table S1). In machine-learning models, the correlation among predictive variables does not affect the model accuracy, as machine-learning can handle multiple correlated predictors. When

variables are correlated, models often employ techniques such as "sharing" or "regularization" to prevent these variables' effects from impeding the model's fit or performance (Chen & Guestrin, 2016; Strobl et al., 2008). Thus, including many predictor variables is appropriate to improve the predictive power of models. This study resampled all variables in EPSG:4326 (World Geodetic System 1984) at 0.05-degree grid resolution. Variables with a higher original pixel resolution were downsampled using a mean aggregation method, and variables with a lower original resolution were resampled using simple upsampling to align with the 0.05-degree grid resolution.

Eight long-term (1981–2010) climate variables were from the Climatologies at High resolution for the Earth Land Surface Areas (CHELSA V2.1) (Karger et al., 2021). Soil property variables for soil organic carbon, total nitrogen, bulk density, sand proportion, pH, and organic carbon density were derived from the SoilGrids250m 2.0 (Hengl et al., 2017). Yearly gross primary production and net primary production were extracted from GLASS products (1982–2018) (Liang et al., 2021), and yearly estimates of the Normalized Difference Vegetation Index are based on the AVHRR product (1982–2019) (Parente & Hengl, 2020). To incorporate vegetation type as a predictor in subsequent analyses, we standardized the classification of vegetation types using the European Space Agency Climate Change Initiative (ESACCI) data product (Harper et al., 2023). This involved harmonizing the classes across the metadata and the vegetation type gridded variables based on the original description and geographic locations of the sampling sites from the retrieved papers (Figure S2; Table S3). The soil microbial biomass carbon was from Xu et al. (2013). Soil fauna diversity was derived from the European Soil Data Centre (ESDAC) (Serna-Chavez et al., 2013).

2.4 | Modeling

We applied the machine-learning techniques RF, GBM, and XGB to fit global models of foliar litter carbon release rate. RF is an ensemble learning method that builds a large collection of decision trees and outputs average predictions of the individual regression trees (Krzywinski & Altman, 2017). GBM's sequential tree-building approach enables robust handling of multicollinearity and increased resilience to outliers, as each tree focuses on capturing errors from previous trees, adapting to complex variable relationships (Appelhans et al., 2015). XGB is an ensemble model consisting of decision trees trained sequentially by fitting the residual errors in each iteration (Chen & Guestrin, 2016). It effectively addresses multicollinearity using regularization techniques and has the capability to capture nonlinear relationships, automatically detecting complex interactions among covariates. The decomposition rates of the foliar litter were logarithmically transformed to reduce the skewness of distributions, and the amount of variation explained by the model after log-transformation was reported (Figure S3a). Prior to running models for a specific problem, it is commonly recommended to optimize a set of tuning parameters, known as hyperparameters, which cannot be directly estimated from the data. These hyperparameters



play a crucial role in determining the training strategy and algorithm efficiency, aiming to maximize model performance. To accomplish this, we used the “train” function from the R package “caret” to optimize the tuning parameters for the models employed in this study. Repeated random cross-validation was performed, and the hyperparameters resulting in the lowest root mean square error (RMSE) were selected (Table S2; Figure S3b-d).

2.5 | Model test and uncertainty

For the accuracy assessment of models, we used a method to define the area of applicability of predictions by comparing the dissimilarity index (DI; based on the distance of each grid location to its nearest neighbors in multi-dimensional space) to a DI value of in the training data (Meyer & Pebesma, 2021; Patoine et al., 2022). Locations with DI values exceeding the threshold (0.95) are considered to require cautious interpretation. The results indicated that regions with lower confidence in predictions were mainly located in the high latitudes of the Northern Hemisphere and desert areas of North Africa (Figure S4). These regions currently have limited observed data currently and require further study. We employed a 10-fold repeated cross-validation approach. This involved training the model 10 times using a 90% subset of the data, with the remaining 10% held back for validation. The RMSE and the coefficient of determination (R^2) were then used to quantify the amount of variation explained by the model. R^2 was calculated as (Hengl et al., 2017):

$$R^2 = (1 - SSE / SST) \times 100\%, \quad (4)$$

where SSE is the sum of the squared error between observation and prediction, and SST is the total sum of squares. To get the per-pixel mean and standard deviation, and estimate the relative importance of each covariate, we performed 100 iterations of the model using the same tuning parameters and then averaged the model results (Figure S5). Then, we calculated the coefficient of variation (standard deviation divided by the mean predicted value) as a measure of the prediction variability of our models (Figure S6). Besides predictions based on individual models, we employed an ensemble prediction procedure. This method averages the predictions generated by models fitted by different techniques weighted by model accuracy (the inverse of the model squared error) from the random cross-validation process.

2.6 | Foliar litter carbon residence time projection

To project the potential foliar litter carbon residence time changes to climate change, we used the predicted climate datasets (MAT: mean annual temperature, BIO_2: mean diurnal range, BIO_3: Isothermality, BIO_4: temperature seasonality, MAP: mean annual precipitation, BIO_13: precipitation of wettest month, BIO_14: precipitation of driest month, BIO_15: precipitation seasonality) for the three periods (2011–2040, 2041–2070 and 2071–2100) obtained from five global climate models (GFDL-ESM4, IPSL-CM6A-LR, MPI-ESM1-2HR,

MRI-ESM2-0 and UKESM1-0-LL) under the SSP 1–2.6 and SSP 5–8.5 scenario. The data are available at the CHELSA (Karger et al., 2017) (<https://chelsa-climate.org/downloads>). CHELSA adopts an approach of preselecting GCMs and SSP, aligning with the models specified by the Intersectoral Impact Model Intercomparison Project (ISIMIP). In the SSP 1–2.6 scenario, the global MAT are projected to increase by 1.36, 2.13, and 2.17°C in each future period, respectively, relative to the long-term MAT (1981–2010). In the SSP 5–8.5 scenario, the corresponding increases are projected to be 1.45, 3.43, and 5.97°C, respectively (Figure S7; Table S4). In the SSP 1–2.6 scenario, MAP changes range from -315 mm to +705 mm, while in the SSP 5–8.5 scenario, MAP varies from -1282 to +1434 mm. Precipitation changes are unevenly distributed, with noticeable decreases in precipitation around the Mediterranean and Amazon regions (Figure S8). We only investigated the impact of temperature and precipitation changes on the rate of carbon release from litter decomposition, keeping other predictors constant. For example, we did not include models on how climate change affects vegetation distribution, changes in land surface area due to sea level rise, or variations in microbial biomass. We acknowledge that the future land-use and climate change will have significant consequences for biodiversity (Brondízio et al., 2019; Pereira et al., 2024), which are likely to modulate decomposition rates and need to be addressed in future work. All analyses were performed in R version 4.3.1 (R Core Team, 2023). The primary packages used in the study were as follows: caret, raster, ranger, xgboost, tidyverse, ggplot2, dplyr, doParallel, foreach, cowplot.

3 | RESULTS AND DISCUSSION

3.1 | Global biogeography of foliar litter carbon release rate

Using the observation-based decomposition dataset and machine-learning models, we derived a global mean k of 0.69 year^{-1} (95% CI: 0.22 – 1.95 year^{-1}). Globally, the spatial variation of k observed in our analysis spans almost two orders of magnitude, ranging from 0.09 to 5.6 year^{-1} . The highest rates of litter carbon release occurred near the equator, spanning the Amazon Plain, the Congo Basin, the Indian Peninsula, and the Southeast Asian Archipelago (Figure 1b). The vegetation in these regions, as defined by the ESACCI, consists of broadleaved forests, except for the Indian Peninsula, where the predominant vegetation type is cropland (Figure S2). Conversely, the slowest rate of decomposition was predicted in the high latitudes of North America, near the Arctic, and the high altitudes on the Tibetan Plateau (Figure 1b). These areas correspond to vegetation types of lichen-moss and grassland, respectively. The predicted pattern of k aligns with the current understanding of the decomposition rate distribution, being faster in regions with higher temperature and moisture. This further elucidates a strong vegetation and climate dependence across large spatial scales (Canessa et al., 2021; Zanne et al., 2022).

Depending on the release rate, we calculated the time required for the release of 50% ($\tau_{50\%}$) and 95% ($\tau_{95\%}$) of litter carbon mass

to reflect the residence time. Residence times exhibited significant variation with latitude, with $\tau_{50\%}$ being 0.58 year in the equatorial tropics and 2.63 year (mean τ above 70°N) in the high northern latitudes (Figure 1c). The difference in latitude for $\tau_{95\%}$ was more pronounced, with 2.49 and 11.38 year in these two regions, respectively (Figure 1d). Across all latitudes, we observed that the mean $\tau_{50\%}$ and $\tau_{95\%}$ are 1.43 and 6.18 year, respectively, with comparatively minor variations in $\tau_{50\%}$ (Figure S9). In the Northern Hemisphere, the most rapid latitudinal increase occurred between the temperate zones (between 55° and 60°N) and the tropical zones (between 15° and 20°N). The Arctic Circle exhibited the longest residence time, with obvious variation among the three predicted models (Figure 1c,d). This divergence could be attributed to the correlation between low MAT and release rate inherent in each model (Figure S10). In latitudes greater than 50°S, there was a significant decrease in τ due to changes in the altitude and vegetation types of southern South America (Figure 2d). Overall, the latitude variation of litter carbon τ showed a pronounced latitudinal asymmetry between the Northern and Southern Hemispheres, resulting from the integrated effects of vegetation types and climate variables.

3.2 | Vegetation-level patterns of foliar litter carbon release

Our study demonstrated that, on the global scale, the vegetation type was the most important predictor for the rate of foliar litter carbon release in each model (Figure 2a). In the longstanding hierarchical paradigm, climate is considered the predominant control, taking the spotlight in the conceptual framework of litter decay studies (Joly et al., 2023; Swift et al., 1979). However, recent research has revealed the inadequacy of the climate-centered view at regional scales (Bradford et al., 2014, 2017). Without delving into the intricate role of the relative importance among various environmental factors, our findings indicated that vegetation type stands out as an integrated proxy for litter decomposition. On the one hand, the decomposability of litter, characterized by indicators such as lignin, nitrogen, and phosphorus nutrient concentrations (i.e., litter quality), governs the priority of litter consumption by decomposers (Bradford et al., 2016). Higher quality litter (higher nitrogen, lower lignin content) implies a faster decomposition (Cotrufo et al., 2013) and higher energy availability of the compounds with regular structures

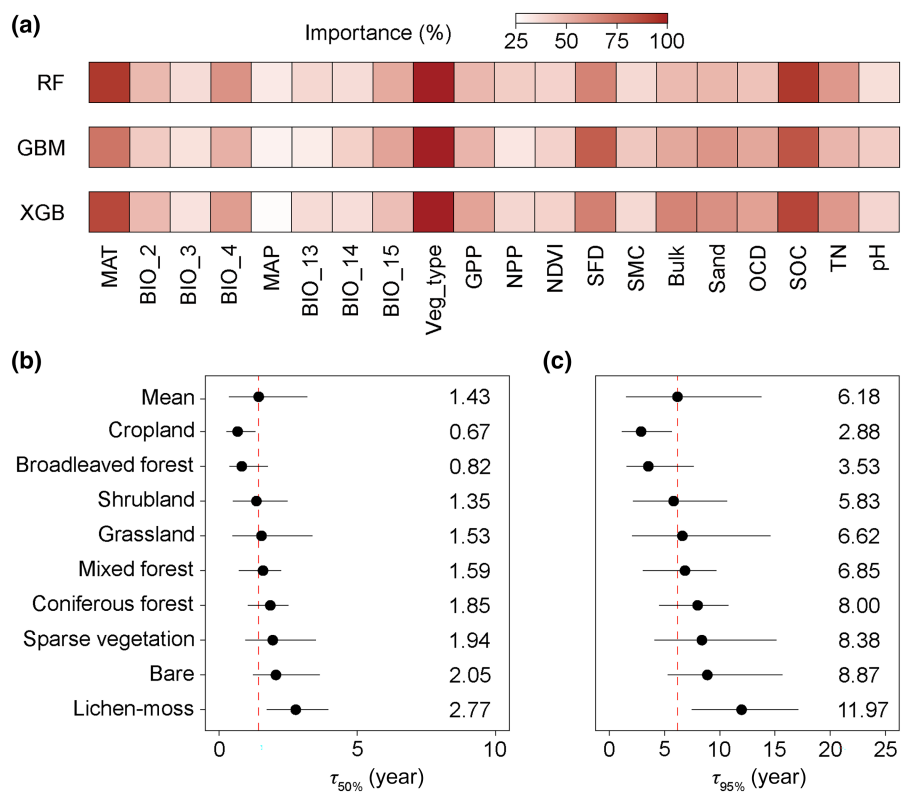


FIGURE 2 Variable importance and vegetation patterns of foliar litter carbon residence time (τ). (a) Variable importance from 100 runs of each model, calculated by the mean decrease in accuracy after variable permutation. Variables were ordered by the median values. BIO_13, precipitation of wettest month; BIO_14, precipitation of driest month; BIO_15, precipitation seasonality; BIO_2, mean diurnal range; BIO_3, isothermality; BIO_4, temperature seasonality; Bulk, soil bulk density; GBM, gradient boosting machine; GPP, gross primary production; MAP, mean annual precipitation; MAT, mean annual temperature; NDVI, normalized difference vegetation index; NPP, net primary production; OCD, soil organic carbon density; pH, soil pH; RF, random forest; Sand, soil sand content; SFD, soil fauna diversity; SMC, soil microbial biomass carbon; SOC, soil organic carbon content; TN, soil total nitrogen content; Veg_type, Vegetation type; XGB, extreme gradient boosting. (b, c) Vegetation trends in τ of foliar litter carbon. Data estimates of τ were aggregated by vegetation types and the ranges reported are the 2.5th (P 2.5) and 97.5th (P 97.5) percentiles, which can be interpreted as the confidence intervals in these estimates. The dotted red line represents the global average of τ , with $\tau_{50\%}$ and $\tau_{95\%}$ being 1.43 and 6.18 year, respectively.

(cellulose, hemicellulose, proteins) (Gunina & Kuzyakov, 2022). On the other hand, the type and phylogenetic structure of litter correspond to specific natural vegetation types in particular sites, shaped by long-term adaptation and evolution (Mori et al., 2020; Pietsch et al., 2014).

When examined by vegetation type, cropland exhibited the shortest residence times, with mean $\tau_{50\%}$ and $\tau_{95\%}$ of 0.67 and 2.88 year, respectively (Figure 2b,c; Figure S11a). This may be attributed to the long-term impact of cultivation practices and fertilization in cropland. Meanwhile, cropland was widely distributed across multiple climate zones (Figure S2), with the highest variations ($\tau_{95\%}$ 95% CI: 2.07–14.95 year). The longest residence times were found in lichen-moss systems located within the Arctic Circle, with mean $\tau_{50\%}$ and $\tau_{95\%}$ of 2.77 and 11.97 year, respectively (Figure 2b,c). The τ of broadleaf forests ($\tau_{50\%}$: 0.82 year, $\tau_{95\%}$: 3.53 year) was much shorter than that of mixed forests ($\tau_{50\%}$: 1.59 year, $\tau_{95\%}$: 6.85 year) and coniferous forests ($\tau_{50\%}$: 1.85 year, $\tau_{95\%}$: 8.00 year). Vegetation types with pronounced moisture constraints such as sparse vegetation and bare areas had a relatively long $\tau_{95\%}$ (8.38 and 8.87 year, respectively) across the entire range of environmental temperatures (Figure S11h,i). Considering the carbon release rates of litter types and their distribution in temperature and precipitation (Figure S11), our results demonstrated that vegetation type could serve as a proxy, for both litter quality and climate conditions (as opposed to the use of individual climatic

variables such as temperature or precipitation). As a result, our models accurately predicted litter carbon τ based on vegetation types and their respective climate zones.

The reader should note the importance of considering potential comparability issues regarding the estimated litter release rates and residence time derived from the extensive field site data on foliar litter carbon decomposition across locations and durations. We therefore used single exponential models to calculate decay rates for the comparison across different experiments, as done in previous studies (e.g., Rovira & Rovira, 2010; Zanne et al., 2022). Notably, the dataset collected for this study encompasses experimental durations ranging from months to years, and represents one of the most comprehensive datasets available on foliar litter carbon release to date.

3.3 | Responses of foliar litter carbon residence time to climate change

We projected the changes of τ under the CMIP6 (Eyring et al., 2016) SSP 1–2.6 and SSP 5–8.5 scenarios during the periods 2011–2040, 2041–2070, and 2071–2100 (hereafter referred to as 2040, 2070, and 2100, respectively). The MAT exhibited varying degrees of increase across different periods (ranging between 1.36 to 5.97°C, Table S4). The foliar litter carbon τ decreased by 2.7% and 5.9% in 2100 (Figure 3) under SSP 1–2.6 and SSP 5–8.5, respectively

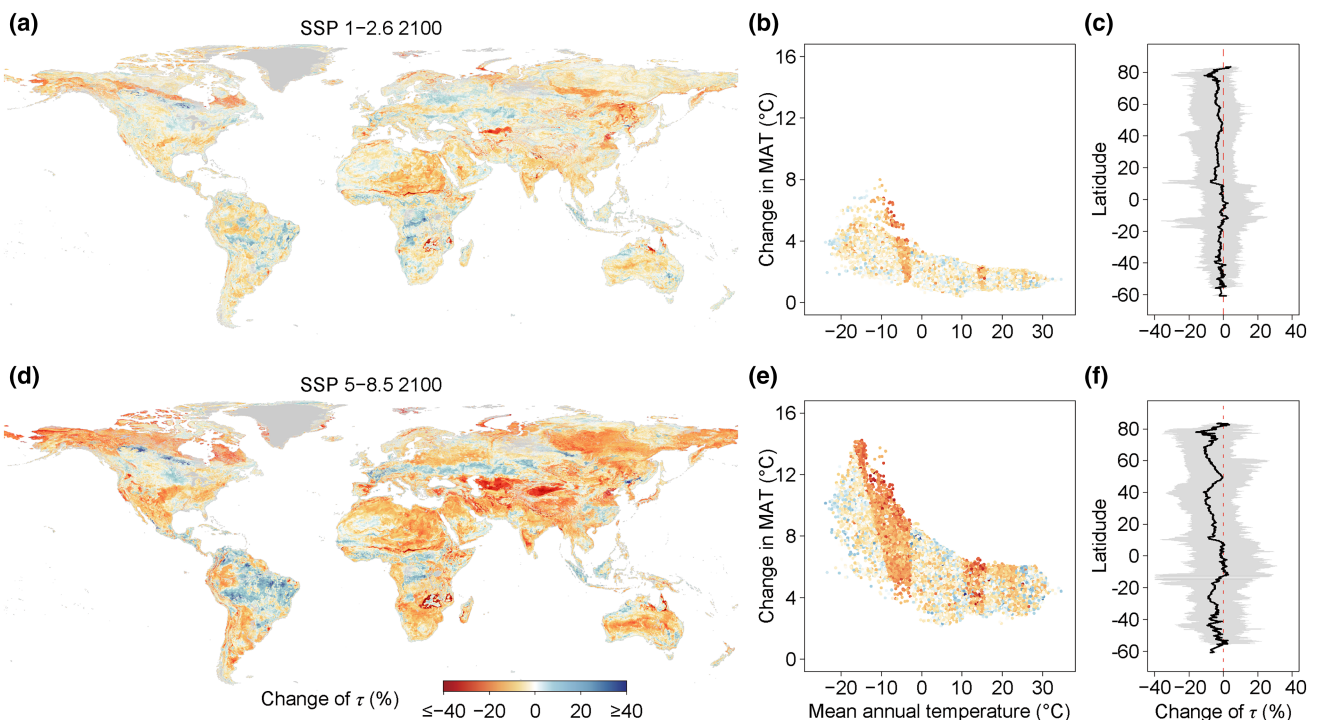


FIGURE 3 Global distributions and latitudinal patterns of change of foliar litter carbon residence time (τ) under different climate projections. Predicted changes of τ , under weaker climate change scenarios (a–c SSP 1–2.6) and stronger climate change scenarios (d–f SSP 5–8.5), show an average decrease of 2.7% and 5.8%, respectively. The results based on the data from CHELSA V2.1 and CMIP6 forecasts for period 2071–2100. Change in MAT is relative to the mean of 1981–2010 baseline (°C). The forecast results for period 2011–2040 and 2041–2070 can be found in Figures S12 and S13. CHELSA, Climatologies at High resolution for the Earth Land Surface Areas; MAT, mean annual temperature; SSP, Shared Socioeconomic Pathway.

(2040: 1.7% and 1.7%, 2070: 2.6% and 3.9%, [Figures S12 and S13](#)). It is evident that the magnitude of global mean τ change is positively correlated with temperature increases ([Figure 4a](#)). Meanwhile, predictions across all scenarios consistently demonstrated an overall increase of litter carbon τ in extremely arid and cold climatic zones, particularly in regions near the Arctic, as well as above the 60°N latitude ([Figure 3a,d](#)). In areas with MAT ranging from -5 to -15°C, litter carbon τ notably decreased by more than 20%. This asymmetrical response was amplified under SSP 5-8.5 compared to SSP 1-2.6 ([Figure 3b,e](#)). Our analysis supports the concern that rising temperatures speed up the carbon loss from litter to soil or atmosphere, especially in cold biomes with slower carbon turnover times (Carvalhais et al., [2014](#)), potentially leading to a positive litter carbon-climate feedback that could, in turn, exacerbate warming (Zhang et al., [2021](#)). In regions

with a MAT of around 15°C, τ also showed a strong decrease (from 2% to 15%) ([Figure 3b,e](#)). This region primarily encompasses the extremely arid areas of northern tropical Africa and Central Asia ([Figure 3a,d](#)). The simultaneous increase in temperature and increased precipitation in the future accelerates the release of litter carbon in such area ([Figure S8](#)).

With increasing warming, mean τ decreased more markedly, revealing distinctions between vegetation types ([Figure 4b](#)). In cold biomes, like lichen-moss systems, the reduction of mean τ was most pronounced, reaching up to 9.6% (equivalent to 1 year) in the 2100 period under SSP 5-8.5 ([Figure 4b; Table S5](#)). A high northern latitude, characterized by extensive permafrost, introduce considerable uncertainty regarding both the impact of warming on microbial utilization efficiency and the soil organic carbon cycle following the accelerated release of litter carbon. Our results showed that in arid regions, specifically in bare areas, a slight increase in precipitation (MAP increasing by 20mm) led to a notable reduction of over 5% in mean τ during the 2100 period ([Figure 4b; Figure S8](#)). In all scenarios across different vegetation types, broadleaf forest showed the smallest response, with a respective decrease of 0.8% and 2.0% under SSP 1-2.6 and SSP 5-8.5 in the period 2100, respectively ([Figure 4b](#)). Furthermore, we noted that a 4.6% increase (95% CI: -13.7 to 25.1) in mean τ of broadleaf forests in the Amazon tropical region might be attributed to a decrease in MAP (over 100mm) under SSP 5-8.5 ([Figure 4b; Figure S8](#)). These results suggest that water conditions modulate variations in τ in warm climates, conversely, temperature controls that in cold climates. Therefore, temperature and precipitation are both important in shaping the spatial and temporal patterns of carbon release response (Fan et al., [2022](#)). Our analysis is limited to temperature and precipitation change, and adaptation of vegetation and decomposer to drier or wetter conditions includes leaf sclerophyll, long leaf lifespans, and higher carbon use efficiency (Joswig et al., [2022](#); Tao et al., [2023](#)), which together lead to uncertainty of turnover times. Thus, it is crucial to consider the effects of climate and other factors over time, ensuring the applicability of models.

In conclusion, the globally compiled foliar litter experimental data enables us to present an observation-based estimate of the carbon release rate and capture global patterns of the litter carbon release in response to climate change. Our results offer, for the first time, explicit quantitative information on litter carbon decomposition rate at the global scale, enhancing the accuracy of identifying carbon fluxes between land and atmosphere in Earth system models. Specifically, estimates from our study can be parameterized in terrestrial carbon cycle models, avoiding the use of mean fixed parameters within previous models. Our results highlight that vegetation type, the proxy of decomposability and biomes, effectively accounts for the carbon release rate of foliar litter. In the context of climate change, global foliar carbon release is accelerating, with faster rates in cold regions due to rising temperatures. Meanwhile, changes in decomposition rates in warm regions exhibit a positive correlation with variations in precipitation. Moving forward, more attention must be paid to understudied regions currently experiencing limited

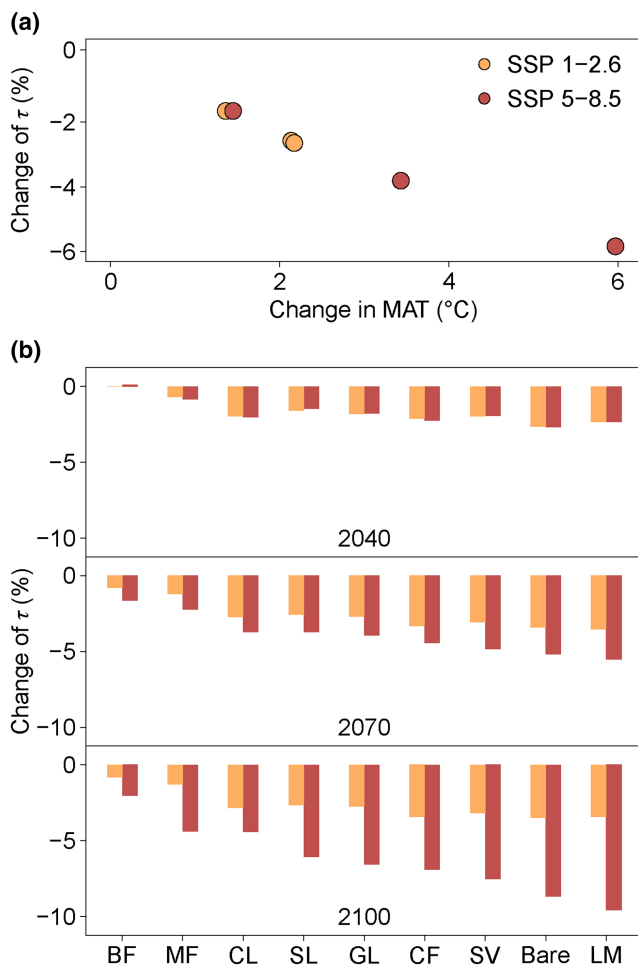


FIGURE 4 Change of mean residence time (τ) under two climate warming scenarios (SSP 1-2.6 and SSP 5-8.5). (a) Forecast decreases in global mean τ by 2040, 2070 and 2100 period versus forecast mean warming relative to a historical baseline (1981–2010). (b) Change of mean τ of each vegetation type under three forecast period. Bare, bare area; BF, broadleaved forest; CF, coniferous forest; CL, cropland; GL, grassland; LM, lichen-moss; MF, mixed forest; SL, shrubland; SSP, Shared Socioeconomic Pathway; SV, sparse vegetation.

decomposition rates but greater climate-change responses, such as extremely cold and arid environments, to better understand their responses to climate change.

AUTHOR CONTRIBUTIONS

Zihao Chen: Conceptualization; data curation; methodology; visualization; writing – original draft; writing – review and editing. **Xiangyin Ni:** Conceptualization; funding acquisition; writing – original draft; writing – review and editing. **Guillaume Patoine:** Methodology; visualization; writing – original draft; writing – review and editing. **Changhui Peng:** Methodology; writing – review and editing. **Kai Yue:** Methodology; writing – original draft; writing – review and editing. **Ji Yuan:** Methodology; visualization; writing – original draft; writing – review and editing. **Qiuxia Wu:** Data curation; methodology; writing – original draft; writing – review and editing. **Nico Eisenhauer:** Writing – original draft; writing – review and editing. **Carlos A. Guerra:** Writing – original draft; writing – review and editing. **Roland Bol:** Methodology; writing – review and editing. **Fuzhong Wu:** Conceptualization; methodology; writing – original draft; writing – review and editing. **G. Geoff Wang:** Writing – review and editing.

ACKNOWLEDGEMENTS

This study was supported by the National Key R&D Program of China (2023YFF1305500), National Natural Science Foundation of China (32022056), and National Natural Science Foundation of China (32171641). G.P., C.A.G., and N.E. acknowledge support of iDiv funded by the German Research Foundation (DFG-FZT 118, 202548816). N.E. also acknowledges support by the DFG (Ei 862/29-1; Ei 862/31-1).

CONFLICT OF INTEREST STATEMENT

The authors declare no competing interests.

DATA AVAILABILITY STATEMENT

The data that support the findings of this study are available in Zenodo at <https://zenodo.org/records/11192456>. The global gridded datasets used in this study as environmental covariates are available in the public domain (see Table S1 for a full list). *Code availability:* All the code used in the analyses presented in this paper is available via <https://zenodo.org/records/11192456> in the code folder.

ORCID

- Zihao Chen  <https://orcid.org/0000-0002-9029-6444>
Xiangyin Ni  <https://orcid.org/0000-0002-2507-3463>
Guillaume Patoine  <https://orcid.org/0000-0002-3748-6644>
Changhui Peng  <https://orcid.org/0000-0003-2037-8097>
Kai Yue  <https://orcid.org/0000-0002-7709-8523>
Ji Yuan  <https://orcid.org/0000-0002-8431-7341>
Nico Eisenhauer  <https://orcid.org/0000-0002-0371-6720>
Carlos A. Guerra  <https://orcid.org/0000-0003-4917-2105>
Roland Bol  <https://orcid.org/0000-0003-3015-7706>
Fuzhong Wu  <https://orcid.org/0000-0003-0411-5908>
G. Geoff Wang  <https://orcid.org/0000-0002-1468-4859>

REFERENCES

- Appelhans, T., Mwangomo, E., Hardy, D. R., Hemp, A., & Nauss, T. (2015). Evaluating machine learning approaches for the interpolation of monthly air temperature at Mt. Kilimanjaro, Tanzania. *Spatial Statistics*, 14, 91–113.
Berg, B. (2014). Decomposition patterns for foliar litter—A theory for influencing factors. *Soil Biology and Biochemistry*, 78, 222–232.
Berg, B., & McClaugherty, C. (2014). *Plant litter: Decomposition, humus formation, carbon sequestration* (3rd ed.). Springer.
Bradford, M. A., Berg, B., Maynard, D. S., Wieder, W. R., & Wood, S. A. (2016). Understanding the dominant controls on litter decomposition. *Journal of Ecology*, 104(1), 229–238.
Bradford, M. A., Tordoff, G. M., Eggers, T., Jones, T. H., & Newington, J. E. (2002). Microbiota, fauna, and mesh size interactions in litter decomposition. *Oikos*, 99(2), 317–323.
Bradford, M. A., Veen, G. F., Bonis, A., Bradford, E. M., Classen, A. T., Cornelissen, J. H. C., Crowther, T. W., De Long, J. R., Freschet, G. T., Kardol, P., Manrubia-Freixa, M., Maynard, D. S., Newman, G. S., Logtestijn, R. S. P., Viktoft, M., Wardle, D. A., Wieder, W. R., Wood, S. A., & Van Der Putten, W. H. (2017). A test of the hierarchical model of litter decomposition. *Nature Ecology & Evolution*, 1, 1836–1845.
Bradford, M. A., Warren, I. R., Baldrian, P., Crowther, T. W., Maynard, D. S., Oldfield, E. E., Wieder, W. R., Wood, S. A., & King, J. R. (2014). Climate fails to predict wood decomposition at regional scales. *Nature Climate Change*, 4, 625–630.
Brondizio, E. S., Settele, J., Diaz, S., & Ngo, H. T. (Eds.). (2019). *The global assessment report of the intergovernmental science-policy platform on biodiversity and ecosystem services*. Intergovernmental Science-Policy Platform on Biodiversity and Ecosystem Services (IPBES).
Cai, L., Kreft, H., Taylor, A., Denelle, P., Schrader, J., Essl, F., Van Kleunen, M., Pergl, J., Pyšek, P., Stein, A., Winter, M., Barcelona, J. F., Fuentes, N., Inderjit, Karger, D. N., Kartesz, J., Kuprijanov, A., Nishino, M., Nickrent, D., ... Weigelt, P. (2023). Global models and predictions of plant diversity based on advanced machine learning techniques. *New Phytologist*, 237(4), 1432–1445.
Canessa, R., Brink, L., Saldaña, A., Rios, R. S., Hättenschwiler, S., Mueller, C. W., Prater, I., Tielbörger, K., & Bader, M. Y. (2021). Relative effects of climate and litter traits on decomposition change with time, climate and trait variability. *Journal of Ecology*, 109(1), 447–458.
Carvalhais, N., Forkel, M., Khomik, M., Bellarby, J., Jung, M., Migliavacca, M., Mu, M., Saatchi, S., Santoro, M., Thurner, M., Weber, U., Ahrens, B., Beer, C., Cescatti, A., Randerson, J. T., & Reichstein, M. (2014). Global covariation of carbon turnover times with climate in terrestrial ecosystems. *Nature*, 514, 213–217.
Chen, T., & Guestrin, C. (2016). XGBoost: A scalable tree boosting system. In *Proceedings of the 22nd ACM SIGKDD international conference on knowledge discovery and data mining* (pp. 785–794).
Cotrufo, M. F., Wallenstein, M. D., Boot, C. M., Denef, K., & Paul, E. (2013). The microbial efficiency-matrix stabilization (MEMS) framework integrates plant litter decomposition with soil organic matter stabilization: Do labile plant inputs form stable soil organic matter? *Global Change Biology*, 19(4), 988–995.
Djurkic, I., Kepfer-Rojas, S., Schmidt, I. K., Larsen, K. S., Beier, C., Berg, B., Verheyen, K., Caliman, A., Paquette, A., Gutiérrez-Girón, A., Humber, A., Valdecantos, A., Petraglia, A., Alexander, H., Augustaitis, A., Saillard, A., Fernández, A. C., Sousa, A. I., Lillebø, A. I., ... Tóth, Z. (2018). Early stage litter decomposition across biomes. *Science of the Total Environment*, 628–629, 1369–1394.
Eyring, V., Bony, S., Meehl, G. A., Senior, C. A., Stevens, B., Stouffer, R. J., & Taylor, K. E. (2016). Overview of the Coupled Model Intercomparison Project Phase 6 (CMIP6) experimental design and organization. *Geoscientific Model Development*, 9(5), 1937–1958.

- Fan, N., Reichstein, M., Koirala, S., Ahrens, B., Mahecha, M. D., & Carvalhais, N. (2022). Global apparent temperature sensitivity of terrestrial carbon turnover modulated by hydrometeorological factors. *Nature Geoscience*, 15, 989–994.
- Farina, R., Coleman, K., & Whitmore, A. P. (2013). Modification of the RothC model for simulations of soil organic C dynamics in dryland regions. *Geoderma*, 200–201, 18–30.
- García-Palacios, P., Maestre, F. T., Kattge, J., & Wall, D. H. (2013). Climate and litter quality differently modulate the effects of soil fauna on litter decomposition across biomes. *Ecology Letters*, 16(8), 1045–1053.
- Gunina, A., & Kuzyakov, Y. (2022). From energy to (soil organic) matter. *Global Change Biology*, 28(7), 2169–2182.
- Harper, K. L., Lamarche, C., Hartley, A., Peylin, P., Ottlé, C., Bastrikov, V., San Martín, R., Bohnenstengel, S. I., Kirches, G., Boettcher, M., Shevchuk, R., Brockmann, C., & Defourny, P. (2023). A 29-year time series of annual 300 m resolution plant-functional-type maps for climate models. *Earth System Science Data*, 15(3), 1465–1499.
- Hengl, T., Mendes de Jesus, J., Heuvelink, G. B. M., Ruiperez Gonzalez, M., Kilibarda, M., Blagotić, A., Shangguan, W., Wright, M. N., Geng, X., Bauer-Marschallinger, B., Guevara, M. A., Vargas, R., MacMillan, R. A., Batjes, N. H., Leenaars, J. G. B., Ribeiro, E., Wheeler, I., Mantel, S., & Kempen, B. (2017). SoilGrids250m: Global gridded soil information based on machine learning. *PLoS One*, 12(2), e0169748.
- Joly, F.-X., Scherer-Lorenzen, M., & Hättenschwiler, S. (2023). Resolving the intricate role of climate in litter decomposition. *Nature Ecology & Evolution*, 7, 214–223.
- Joswig, J. S., Wirth, C., Schuman, M. C., Kattge, J., Reu, B., Wright, I. J., Sippel, S. D., Rüger, N., Richter, R., Schaeppman, M. E., van Bodegom, P. M., Cornelissen, J. H. C., Díaz, S., Hattingh, W. N., Kramer, K., Lens, F., Niinemets, Ü., Reich, P. B., Reichstein, M., ... Mahecha, M. D. (2022). Climatic and soil factors explain the two-dimensional spectrum of global plant trait variation. *Nature Ecology & Evolution*, 6, 36–50.
- Karger, D. N., Conrad, O., Böhner, J., Kawohl, T., Kreft, H., Soria-Auza, R. W., Zimmermann, N. E., Linder, H. P., & Kessler, M. (2017). Climatologies at high resolution for the earth's land surface areas. *Scientific Data*, 4(1), 170122.
- Karger, D. N., Wilson, A. M., Mahony, C., Zimmermann, N. E., & Jetz, W. (2021). Global daily 1 km land surface precipitation based on cloud cover-informed downscaling. *Scientific Data*, 8(1), 307.
- Krzywinski, M., & Altman, N. (2017). Classification and regression trees. *Nature Methods*, 14(8), 757–758.
- Lajtha, K., Bowden, R. D., Crow, S., Fekete, I., Kotroczo, Z., Plante, A., Simpson, M. J., & Nadelhoffer, K. J. (2018). The detrital input and removal treatment (DIRT) network: Insights into soil carbon stabilization. *Science of the Total Environment*, 640–641, 1112–1120.
- Lehmann, J., & Kleber, M. (2015). The contentious nature of soil organic matter. *Nature*, 528, 60–68.
- Li, S., Yuan, W., Ciais, P., Viovy, N., Ito, A., Jia, B., & Zhu, D. (2019). Benchmark estimates for aboveground litterfall data derived from ecosystem models. *Environmental Research Letters*, 14(8), 084020.
- Liang, S., Cheng, J., Jia, K., Jiang, B., Liu, Q., Xiao, Z., Yao, Y., Yuan, W., Zhang, X., Zhao, X., & Zhou, J. (2021). The global land surface satellite (GLASS) product suite. *Bulletin of the American Meteorological Society*, 102(2), E323–E337.
- Luo, Y., & Schuur, E. A. G. (2020). Model parameterization to represent processes at unresolved scales and changing properties of evolving systems. *Global Change Biology*, 26(3), 1109–1117.
- Meyer, H., & Pebesma, E. (2021). Predicting into unknown space? Estimating the area of applicability of spatial prediction models. *Methods in Ecology and Evolution*, 12(9), 1620–1633. <https://doi.org/10.1111/2041-210X.13650>
- Mori, A. S., Cornelissen, J. H. C., Fujii, S., Okada, K., & Isbell, F. (2020). A meta-analysis on decomposition quantifies afterlife effects of plant diversity as a global change driver. *Nature Communications*, 11, 4547.
- Olson, J. S. (1963). Energy storage and the balance of producers and decomposers in ecological systems. *Ecology*, 44(2), 322–331.
- Pan, Y., Birdsey, R. A., Fang, J., Houghton, R., Kauppi, P. E., Kurz, W. A., Phillips, O. L., Shvidenko, A., Lewis, S. L., Canadell, J. G., Ciais, P., Jackson, R. B., Pacala, S. W., McGuire, A. D., Piao, S., Rautiainen, A., Sitch, S., & Hayes, D. (2011). A large and persistent carbon sink in the world's forests. *Science*, 333(6045), 988–993.
- Parente, L., & Hengl, T. (2020). Monthly global NDVI at 5 km based on AVHRR product—1982 to 2019 (v1.0); Zenodo.
- Parton, W. J., Scurlock, J. M. O., Ojima, D. S., Gilmanov, T. G., Scholes, R. J., Schimel, D. S., Kirchner, T., Menaut, J.-C., Seastedt, T., Garcia Moya, E., Kamnalrut, A., & Kinyamario, J. I. (1993). Observations and modeling of biomass and soil organic matter dynamics for the grassland biome worldwide. *Global Biogeochemical Cycles*, 7(4), 785–809.
- Parton, W., Silver, W. L., Burke, I. C., Grassens, L., Harmon, M. E., Currie, W. S., King, J. Y., Adair, E. C., Brandt, L. A., Hart, S. C., & Fasth, B. (2007). Global-scale similarities in nitrogen release patterns during long-term decomposition. *Science*, 315(5810), 361–364.
- Patoine, G., Eisenhauer, N., Cesarz, S., Phillips, H. R. P., Xu, X., Zhang, L., & Guerra, C. A. (2022). Drivers and trends of global soil microbial carbon over two decades. *Nature Communications*, 13(1), 4195.
- Pereira, H. M., Martins, I. S., Rosa, I. M. D., Kim, H., Leadley, P., Popp, A., Van Vuuren, D. P., Hurtt, G., Quoss, L., Arneth, A., Baisero, D., Bakkenes, M., Chaplin-Kramer, R., Chini, L., Di Marco, M., Ferrier, S., Fujimori, S., Guerra, C. A., Harfoot, M., ... Alkemade, R. (2024). Global trends and scenarios for terrestrial biodiversity and ecosystem services from 1900 to 2050. *Science*, 384(6694), 458–465. <https://doi.org/10.1126/science.adn3441>
- Pichler, M., & Hartig, F. (2023). Machine learning and deep learning—A review for ecologists. *Methods in Ecology and Evolution*, 14(4), 994–1016.
- Pietsch, K. A., Ogle, K., Cornelissen, J. H. C., Cornwell, W. K., Bönnisch, G., Craine, J. M., Jackson, B. G., Kattge, J., Peltzer, D. A., Penuelas, J., Reich, P. B., Wardle, D. A., Weedon, J. T., Wright, I. J., Zanne, A. E., & Wirth, C. (2014). Global relationship of wood and leaf litter decomposability: The role of functional traits within and across plant organs. *Global Ecology and Biogeography*, 23(9), 1046–1057.
- Portillo-Estrada, M., Pihlatie, M., Korhonen, J. F. J., Levula, J., Frumau, A. K. F., Ibrom, A., Lembrechts, J. J., Morillas, L., Horváth, L., Jones, S. K., & Niinemets, Ü. (2016). Climatic controls on leaf litter decomposition across European forests and grasslands revealed by reciprocal litter transplantation experiments. *Biogeosciences*, 13(5), 1621–1633.
- Prescott, C. E. (2010). Litter decomposition: What controls it and how can we alter it to sequester more carbon in forest soils? *Biogeochemistry*, 101(1–3), 133–149.
- Prieto, I., Almagro, M., Bastida, F., & Querejeta, J. I. (2019). Altered leaf litter quality exacerbates the negative impact of climate change on decomposition. *Journal of Ecology*, 107(5), 2364–2382.
- R Core Team. (2023). *A language and environment for statistical computing*. R Foundation for Statistical Computing.
- Rovira, P., & Rovira, R. (2010). Fitting litter decomposition datasets to mathematical curves: Towards a generalised exponential approach. *Geoderma*, 155(3–4), 329–343.
- Serna-Chavez, H. M., Fierer, N., & Van Bodegom, P. M. (2013). Global drivers and patterns of microbial abundance in soil. *Global Ecology and Biogeography*, 22(10), 1162–1172.
- Strobl, C., Boulesteix, A.-L., Kneib, T., Augustin, T., & Zeileis, A. (2008). Conditional variable importance for random forests. *BMC Bioinformatics*, 9(1), 307.
- Swift, M., Heal, O. W., & Anderson, J. (1979). *Decomposition in terrestrial ecosystems*; Blackwell.

- Tao, F., Huang, Y., Hungate, B. A., Manzoni, S., Frey, S. D., Schmidt, M. W. I., Reichstein, M., Carvalhais, N., Ciais, P., Jiang, L., Lehmann, J., Wang, Y.-P., Houlton, B. Z., Ahrens, B., Mishra, U., Hugelius, G., Hocking, T. D., Lu, X., Shi, Z., ... Luo, Y. (2023). Microbial carbon use efficiency promotes global soil carbon storage. *Nature*, 618(7967), 981–985.
- Tuomi, M., Thum, T., Järvinen, H., Fronzek, S., Berg, B., Harmon, M., Trofymow, J. A., Sevanto, S., & Liski, J. (2009). Leaf litter decomposition—Estimates of global variability based on Yasso07 model. *Ecological Modelling*, 220(23), 3362–3371.
- Wang, Z., Yin, X., & Li, X. (2015). Soil mesofauna effects on litter decomposition in the coniferous forest of the Changbai Mountains, China. *Applied Soil Ecology*, 92, 64–71.
- Xu, X., Thornton, P. E., & Post, W. M. (2013). A global analysis of soil microbial biomass carbon, nitrogen and phosphorus in terrestrial ecosystems. *Global Ecology and Biogeography*, 22(6), 737–749.
- Zanne, A. E., Flores-Moreno, H., Powell, J. R., Cornwell, W. K., Dalling, J. W., Austin, A. T., Classen, A. T., Eggleton, P., Okada, K., Parr, C. L., Adair, E. C., Adu-Bredu, S., Alam, A., Alvarez-Garzón, C., Apgaua, D., Aragón, R., Ardon, M., Arndt, S. K., Ashton, L. A., ... Curran, T. J. (2022). Termite sensitivity to temperature affects global wood decay rates. *Science*, 377, 1440–1444.
- Zhang, F., Feng, Y., Song, S., Cai, Q., Ji, C., & Zhu, J. (2021). Temperature sensitivity of plant litter decomposition rate in China's forests. *Ecosphere*, 12(6), e03541.

SUPPORTING INFORMATION

Additional supporting information can be found online in the Supporting Information section at the end of this article.

How to cite this article: Chen, Z., Ni, X., Patoine, G., Peng, C., Yue, K., Yuan, J., Wu, Q., Eisenhauer, N., Guerra, C. A., Bol, R., Wu, F., & Wang, G. G. (2024). Climate warming accelerates carbon release from foliar litter—A global synthesis. *Global Change Biology*, 30, e17350. <https://doi.org/10.1111/gcb.17350>